Magnetic nature of KxCoO2 near the antiferromagnetic phase with x=0.5: Positive muon spin rotation and relaxation

Jun Sugiyama, Yutaka Ikedo, Peter L. Russo, Hiroshi Nozaki, Kazuhiko Mukai, Daniel Andreica, Alex Amato, Maxime Blangero, Claude Delmas

Magnetic nature of K_xCoO_2 near the antiferromagnetic phase with $x=0.5$: Positive muon spin rotation and relaxation

Jun Sugiyama,[1,*] Yutaka Ikedo,[1] Peter L. Russo,[2] Hiroshi Nozaki,[1] Kazuhiko Mukai,[1] Daniel Andreica,[3] Alex Amato,[3] Maxime Blangero,[4] and Claude Delmas[4]

[1]*Toyota Central Research and Development Labs., Inc., Nagakute, Aichi 480-1192, Japan*

[2]*TRIUMF, 4004 Wesbrook Mall, Vancouver, British Columbia, V6T 2A3 Canada*

[3]*Laboratory for Muon-Spin Spectroscopy, Paul Scherrer Institut, 5232 Villigen PSI, Switzerland*

[4]*ICMCB-CNRS, 87 Avenue du Schweitzer, F33608 Pessac Cedex, France*

(Received 18 May 2007; revised manuscript received 8 August 2007; published 11 September 2007)

In order to elucidate the magnetic nature of K_xCoO_2 in the vicinity of $x=0.5$, we have measured positive muon spin rotation and relaxation (μ^+SR) spectra using polycrystalline samples of $x=0.6$, 4/7, and 0.5 in the temperature range between 1.8 and 300 K. A zero-field spectrum suggests the existence of localized but disordered moments below 20 K for the $x=0.6$ sample, whereas the spectra reveal the absence of magnetic moments in the $x=4/7$ sample. Combining our μ^+SR results with the results of resistivity and susceptibility measurements, it is found that the phase boundary between the Curie-Weiss metal and Pauli-paramagnetic metal exists between $x=0.6$ and 4/7. For the rhombohedral $x=0.5$ sample (i.e., β phase), the quasistatic antiferromagnetic (AF) order appears below 58 K ($=T_N$), and the whole sample enters into the AF phase below T_N, as in the case for the hexagonal γ-$K_{0.5}CoO_2$. This suggests that the interplane interaction is most unlikely to be crucial for determining the magnetic nature of the CoO_2 plane. The complex T dependence of the internal AF fields, particularly the drastic change at the charge-order transition temperature ($T_{CO}=20$ K), is qualitatively explained by the change in the muon sites induced by charge order in the CoO_2 planes.

DOI: 10.1103/PhysRevB.76.104412 PACS number(s): 75.30.Kz, 75.50.Ee, 76.75.+i, 75.25.+z

I. INTRODUCTION

The K_xCoO_2 (KCO) system, in which Co ions form a two-dimensional triangular lattice by the connection of edge-sharing CoO_6 octahedra much like the case for Na_xCoO_2 (NCO) system, was recently investigated by several experimental techniques.[1–3] This is because KCO is a good reference material for understanding the nature of NCO, which exhibits a variety of fascinating physical phenomena: unconventional transport properties for NCO with $x\sim0.7$,[4] long-range antiferromagnetic (AF) order with $T_N\sim22$ K for $x\geqslant0.75$,[5–7] two successive transitions ($T_N=87$ K and $T_{CO}=53$ K, where T_{CO} symbolizes the charge-order transition) in $x=0.5$,[8] and superconductivity with $T_c=5$ K for $x=0.35$ and absorbed water.[9]

In contrast to NCO where the doping concentration can usually be set precisely, the K content x is very difficult to control in a wide x range.[10] Indeed, only the KCO with $0.5\leqslant x\leqslant0.6$ is available by conventional solid-state reaction and/or crystal growth techniques. This is probably due to the competition between the size of alkali ions, i.e., the interplane distance and the electrostatic repulsion of the adjacent CoO_2 planes. That is, a smaller distance requires much alkali ions to shield the repulsion between the O ions in the adjacent CoO_2 planes. Because of the unavailability of suitable KCO materials, the overall picture of the magnetism of the CoO_2 plane in KCO is still unknown, particularly in the x range above 0.75.

Nonetheless, it was found that hexagonal $K_{0.49}CoO_2$ with a space group $P6_3/mmc$ also undergoes two successive transitions at $T_N\sim60$ K and ~20 K by a positive muon spin spectroscopy (μ^+SR) experiment,[1] while $K_{0.49}CoO_2$ is metallic down to 4 K by both susceptibility (χ) and resistivity (ρ) measurements. Interestingly, the μ^+SR experiment on hexagonal $K_{0.48}CoO_2$ crystals, which clearly exhibit both an AF transition at T_N and a metal-to-insulator transition at T_{CO}, provided an almost equivalent result to that for metallic $K_{0.49}CoO_2$.[11] Furthermore, since the whole T dependences of the internal magnetic field (H_{int}) for both $K_{0.49}CoO_2$ and $K_{0.48}CoO_2$ detected by μ^+SR are similar to that for $Na_{0.5}CoO_2$,[12,13] the microscopic magnetic nature of the CoO_2 plane with the average Co valence of ~3.5 is confirmed to be of a common type for both NCO and KCO. This implies that the AF phase appears in the very narrow x range of KCO, as in the case for NCO,[8] although there is no information on the phase boundary of the AF phase for KCO with $x\sim0.5$.

It should be, however, noted that the interplane distance, i.e., the relevant interaction length scale between the adjacent CoO_2 planes (three-dimensional interaction), also plays a significant role in determining T_N and/or T_{CO} of KCO and NCO with $x\sim0.5$, because the magnitude of T_N (T_{CO}) of KCO is lower by 27 K (33 K) than that of NCO. Here, the interplane distance in KCO with $x\sim0.5$ is about 0.625 nm, whereas that for NCO, it is about 0.556 nm. Furthermore, the a-axis length, i.e., the length of the Co–Co bond in the CoO_2 plane, which determines the two-dimensional interaction, is common for both NCO and KCO. Recent μ^+SR studies on Li_xCoO_2 (LCO) clarified the absence of magnetic order in Li_xCoO_2 with $0.1\leqslant x<1$,[14,15] although the AF and/or charge-order transitions are naturally expected to exist for LCO with $x=0.5$ if the interplane distance is a crucial factor for spin and charge orders.

The K-ordered phase $K_4Co_7O_{14}$ (equivalent to $x=4/7=0.5714\ldots$) was recently synthesized by a conventional solid-state reaction technique together with an additional an-

nealing in an oxygen flow.[16] The ordering of K^+ ions leads to a supercell with $\sqrt{7}a_H \times \sqrt{7}a_H$, where a_H (~0.28 nm) is the a-axis length of the CoO_2 plane in hexagonal setting. Since the $\chi(T)$ curve exhibits a Pauli-paramagnetic behavior and ρ decreases monotonically with decreasing T, $K_4Co_7O_{14}$ is presumably thought to lack magnetic order down to 4.2 K. Furthermore, the K-disordered phase $K_{0.6}CoO_2$, in which K^+ ions are randomly located at the regular K sites, is also available.[10] The ρ measurement showed that $K_{0.6}CoO_2$ is metallic down to 4.2 K, although the $\chi(T)$ curve exhibits a rapid increase with lowering T below 100 K (a Curie-Weiss-like behavior). However, considering the existence of the AF order in metallic $K_{0.49}CoO_2$, we also need to investigate the magnetic nature of KCO with $x=4/7$ and 0.6 by microscopic magnetic measurements to determine the AF region in the phase diagram of KCO.

In addition, it is worth noting that there are two stable phases for KCO with $x=0.5$: one is a hexagonal phase with a space group $P6_3/mmc$ and the other a rhombohedral phase with a space group $R3m$. The former is called P2 or γ phase, while the latter P3 or β phase. For both structures, the K^+ layer is sandwiched by two adjacent CoO_2 planes so as to set K^+ ions at the center of the prism formed by the nearest neighboring six oxygens. The sequence of the stacking of oxygen layers in the γ phase is represented as *A-B-B-A*, while in the β phase, *A-B-B-C-C-A*, where *A*, *B*, and *C* are named similar for the stacking sequence in the face centered cubic close-packed structure.[17] Since γ-$K_{0.5}CoO_2$ is synthesized at ~600 °C, whereas β-$K_{0.5}CoO_2$ is at 450 °C, the γ-phase samples are usually obtained by single crystal growth. Indeed, the $K_{0.49}CoO_2$ and $K_{0.48}CoO_2$ single crystals for our past μ^+SR work were assigned to be the γ phase; from now on, we will call the two crystals as γ-$K_{\sim 0.5}CoO_2$ for simplicity. There are, to the authors' knowledge, no studies on the β phase.

Among several magnetic measurement techniques, μ^+SR is particularly sensitive to the local magnetic environment, because the μ^+ only feels $H_{\rm int}$ due to its nearest neighbors and is specially sensitive to short-range magnetic order, which sometimes appears in low-dimensional systems, while both neutron scattering and χ measurements mainly detect long-range magnetic order; if the correlation length is very short, neutron diffraction peaks broaden and eventually disappear.

Here, we report on both weak (relative to the spontaneous internal fields in the ordered state) transverse-field (wTF) μ^+SR and zero field (ZF) μ^+SR, for polycrystalline γ-KCO samples with $x=0.6$ and 4/7 and a β-$K_{0.5}CoO_2$ sample at temperatures between 1.8 and 300 K. The former method is sensitive to local magnetic order via the shift of the μ^+ spin precession frequency in the applied field and the enhanced μ^+ spin relaxation, while ZF-μ^+SR is uniquely sensitive to weak local magnetic (dis)order in samples exhibiting quasistatic paramagnetic moments.

II. EXPERIMENT

Powder samples of K_xCoO_2 with $x=0.5$, 4/7, and 0.6 were prepared at ICMCB-CNRS by a solid-state reaction technique using reagent grade KOH and Co_3O_4 powders as starting materials. A mixture of KOH and Co_3O_4 was heated at 600 °C for 12 h in a dry-oxygen flow and then furnace cooled down to 300 °C with a rate of 1 °C/min. The preparation and characterization of these samples were reported in greater detail elsewhere.[10,16] The composition of the samples was determined by an induction coupled plasma (ICP) analysis. Powder x-ray diffraction analyses showed that the three samples are almost single phase with a rhombohedral or a hexagonal crystal system. The results of ICP and x-ray diffraction analyses are summarized in Table I. We restrict our studies to KCO with $x=0.5$, 4/7, and 0.6 because of the unavailability of the other compositions.[18]

TABLE I. The composition and lattice parameters of KCO with $x=0.6$, 4/7, and 0.5. The lattice parameters of the $x=0.5$ sample are represented in pseudohexagonal setting.

Nominal x	x by ICP	Space group	a_H (nm)	c_H (nm)
0.6	0.61	$P6_3/mmc$	0.2836(1)	1.242(1)
4/7	0.62[a]	$P6_3/m$	0.7517(1)	1.237(1)
0.5	0.52	$R3m$	0.2828(1)	1.868(1)

[a]Due to a small amount of unreacted KOH phase (3–5 wt %).

Since KCO with $x \sim 0.5$ is highly reactive with water in air, the KCO disk was stored in an Ar-filled glass tube, transferred from Bordeaux to PSI, and then removed into an In-sealed sample cell in a glovebox just before the μ^+SR measurement. The μ^+SR spectra were measured at the πE1-Dolly surface muon beamline at PSI in Switzerland. The experimental setup and techniques were described in detail elsewhere.[19]

χ was measured using a superconducting quantum interference device magnetometer (MPMS, Quantum Design) in the temperature range between 400 and 5 K under magnetic field $H \leqslant 55$ kOe. dc ρ was measured using a four-probe method in the T range between 300 and 4.2 K.

III. RESULTS AND DISCUSSION

A. ρ and χ

Figures 1(a) and 1(b) show the T dependences of ρ and χ for the KCO samples with $x=0.6$, 4/7, and 0.5. The $\rho(T)$ curve clearly shows metallic behavior for the $x=4/7$ and 0.6 samples, while the metal-to-insulator transition occurs at ~60 K for the $x=0.5$ sample. Actually, the $\chi(T)$ curve for the $x=4/7$ sample exhibits Pauli-paramagnetic behavior down to 25 K. A small increase in χ below 25 K with decreasing T is probably due to the effect of magnetic impurities, such as Co_3O_4 ($T_N=33$ K).[20] For KCO with $x=0.6$, as T decreases from 350 K, χ is almost T independent down to ~100 K and then increases rapidly with further decreasing T, indicating the appearance of localized moments. On the other hand, for KCO with $x=0.5$, the $\chi(T)$ curve increases monotonically with decreasing T and then exhibits a broad maximum at 35 K then a minimum at 20 K caused by the AF transition.

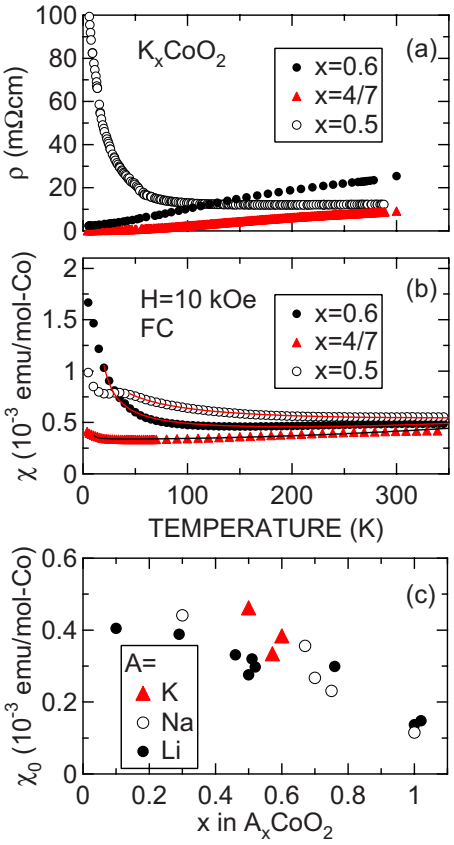

FIG. 1. (Color online) Temperature dependence of (a) resistivity (ρ), (b) susceptibility (χ), and (c) the relationship between the T-independent part of χ (χ_0) and x for KCO with x=0.5, 4/7, and 0.6, together with the results of NCO (Refs. 21 and 22) and LCO (Ref. 15). χ was measured in field-cooling (FC) mode with H =10 kOe. The solid lines in (b) show the fitting results using Eq. (1).

In order to understand the effect of x on electronic structure, the T-independent term of χ (χ_0) was estimated by the general formula

$$\chi(T) = \chi_0(1 + \beta T^2) + \frac{C}{T - \Theta}, \tag{1}$$

$$\beta = \frac{\pi^2 k_B^2}{6}\left[\frac{D''}{D} - \left(\frac{D'}{D}\right)^2\right]_{E=E_F}, \tag{2}$$

where k_B is the Boltzmann constant, D is the density of states at the Fermi level (E_F), D' and D'' are the energy derivative of D, C is the Curie constant, and Θ is the Weiss temperature. The βT^2 term thus comes from the shift of the Fermi level with T in order to explain the positive slope of the $\chi(T)$ curve at high T. The Curie-Weiss (CW) term represents the contribution of the localized moments, regardless if their origin is intrinsic or due to impurities. Note that, in order to know the change in χ_0 with x roughly, we ignored both diamagnetic and orbital contributions to χ_0. However, since $LiCoO_2$ and $NaCoO_2$ are insulators, their χ_0's approximately correspond to the above two contributions for K_xCoO_2. The

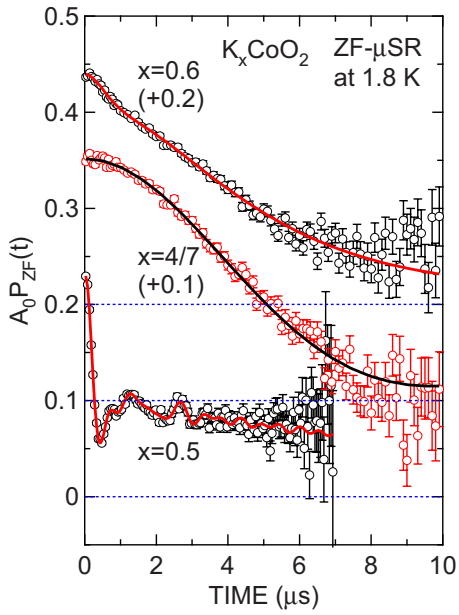

FIG. 2. (Color online) The ZF-μ^+SR time spectra for the three K_xCoO_2 samples at 1.8 K. The solid lines show the fitting results using Eqs. (3), (5), and (6). Each spectrum is offset by 0.1 for clarity of display.

relationship between χ_0 and x is shown in Fig. 1(c), together with the results on NCO[21,22] and LCO.[15] The overall dependence of χ_0 on x for KCO is found to be essentially the same to that of NCO and LCO, although the x range of KCO is very limited. That is, χ_0 increases monotonically with decreasing x, indicating hole doping to the CoO_2 plane by removing alkali ions. Since $\chi_0(x=4/7) < \chi_0(x=0.6)$ for KCO, the K ordering could reduce the interaction between holes. Indeed, the ρ of the x=4/7 sample is the smallest among the present three KCOs [see Fig. 1(a)].

B. μ^+SR

At first, Fig. 2 shows the ZF-μ^+SR spectrum for the three samples at the lowest T measured in order to compare overall changes in the microscopic magnetic nature of KCO with x. For the x=0.6 sample, since there is a change in slope around $t \sim 1$ μs, the spectrum is found to consist of the two relaxation signals (fast and slow), while that for the x=4/7 sample includes only one slow relaxation signal. On the other hand, the spectrum for $K_{0.5}CoO_2$ shows clear oscillations, indicating the appearance of a static H_{int} at low T, as reported for KCO with x=0.49.

1. $K_{0.6}CoO_2$

The ZF spectrum for $K_{0.6}CoO_2$ is hence fitted by a combination of the two Kubo-Toyabe (KT) signals due to randomly oriented magnetic moments,[19]

$$A_0 P_{ZF}(t) = A_{KT1} G^{DGKT}(t, \Delta_1, \nu_1) + A_{KT2} G^{DGKT}(t, \Delta_2, \nu_2), \tag{3}$$

where A_0 is the maximum muon decay asymmetry, A_{KT1} and

TABLE II. The μ^+SR parameters of $K_{0.6}CoO_2$ sample. The data in the first row were obtained by global fitting the ZF and LF spectra using Eq. (3), whereas those in the second and third rows by fitting the ZF spectrum alone.

Fit	T (K)	A_{KT1}	Δ_1 (10^6 s^{-1})	ν_1 (10^6 s^{-1})	A_{KT2}	Δ_2 (10^6 s^{-1})	ν_2 (10^6 s^{-1})
ZF and LF	1.757±0.011	0.032±0.002	1.43±0.02	0.41±0.07	0.207±0.001	0.248±0.001	0.43±0.01
ZF	1.750±0.003	0.036±0.002	1.49±0.08	1.37±0.12	0.203±0.002	0.216±0.011	0.28±0.04
ZF	5.081±0.011	0.036±0.003	2.93±0.10	14.7±0.8	0.205±0.002	0.206±0.009	0.22±0.03

A_{KT2} are the asymmetries of the two dynamic Gaussian-KT signals (G^{DGKT}), Δ_i ($i=1$ and 2) is the static width of the local frequencies at the disordered sites, and ν_i is the field fluctuation rate. When $\nu=0$, $G^{DGKT}(t,\Delta,\nu)$ is the static Gaussian Kubo-Toyabe function $G_{zz}^{KT}(t,\Delta)$.[19]

The results of the global fit using both ZF and longitudinal-field (LF) spectra with LF=50 Oe are listed in Table II together with the result using the ZF spectrum alone. If we ignore a small discrepancy between ν's obtained by the two different fitting methods, the result by global fitting is in good agreement with that by usual fitting, as expected. Since $\Delta_2 \sim 0.2\times10^6$ s^{-1}, the A_{KT2} signal is found to come from muons experiencing solely randomly oriented nuclear magnetic moments, in this case, ^{39}K, ^{40}K, ^{41}K, and ^{59}Co. On the other hand, the muons responsible for the A_{KT1} signal appear to sense also randomly oriented localized electronic moments.

In order to investigate the T dependence of the internal field H_{int} created by these moments in the wide T range, the wTF-μ^+SR spectrum was measured above 5 K under wTF =50 Oe. The spectrum was well fitted by a combination of two oscillatory signals with the same frequency (ω_{TF}) and the initial phase (ϕ) due to an external wTF; that is, one is a relatively fast relaxing component represented by an exponentially relaxation function and the other a slowly relaxing component by a Gaussian-type relaxation. The former relaxation is caused by the appearance of H_{int}, and the latter by the nuclear magnetic moments,

$$A_0 P_{TF}(t) = A_{fast}\exp\left(-\frac{\sigma_{fast}^2 t^2}{2}\right)\cos(\omega_{TF}t+\phi) + A_{TF}\exp\left(-\frac{\sigma_{TF}^2 t^2}{2}\right)\cos(\omega_{TF}t+\phi), \quad (4)$$

where A_{fast} and A_{TF} are the asymmetries of the two signals, and σ_{fast} and σ_{TF} are their respective Gaussian relaxation rates.

Since σ_{TF} is determined by the nuclear magnetic moments and there is no indication for structural phase transitions down to 2 K in the $\rho(T)$ and $\chi(T)$ curves, it is reasonable to assume that σ_{TF} is independent of T if we ignore the effect of thermal expansion on σ_{TF}. The wTF spectra were therefore fitted using a common σ_{TF} in the whole T range below 100 K. Figure 3 shows the T dependences of (a) normalized asymmetries (N_{A_i}), (b) relaxation rates (σ_i), and (c) χ for KCO with $x=0.6$, together with the result of the analysis of the ZF spectrum at 1.8 and 5 K.

As T decreases from 100 K, $N_{A_{TF}}$, which roughly corresponds to the volume fraction (V_F) of paramagnetic (PM) phases in a sample, levels off at its maximum (=1) down to 30 K, decreases monotonically with further decreasing T, and reaches around 0.7 at 1.8 K, suggesting that V_F of the magnetic phase is ~30%. According to the $N_{A_{TF}}(T)$ curve, $N_{A_{fast}}$ has a finite value only below 30 K, increases with decreasing T, and then reaches ~0.3 at 1.8 K. The $\sigma_{fast}(T)$ curve appears below 30 K, accompanies the decrease (in-

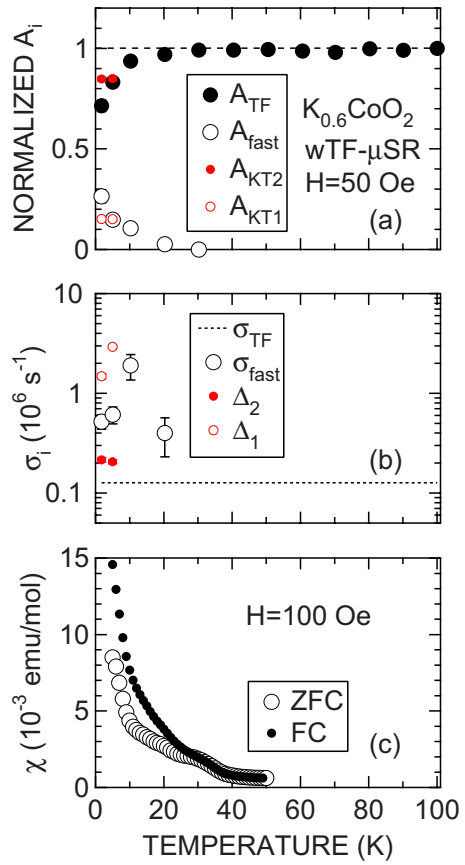

FIG. 3. (Color online) T dependences of (a) normalized asymmetries N_{A_i}, (b) relaxation rates σ_i, and (c) χ for KCO with $x=0.6$. The data were obtained by global fitting the wTF spectra below 100 K using Eq. (4). The broken line in (b) represents σ_{TF} estimated by the global fitting. Small (red) open and solid circles in (a) and (b) represent the data estimated from the ZF spectrum (see Table II). χ was measured both in field-cooling (FC) and zero-field-cooling (ZFC) modes with $H=100$ Oe.

crease) in $N_{A_{TF}}$ ($N_{A_{fast}}$) below 30 K, and exhibits a maximum around 10 K. Note that the analysis of the ZF spectrum provides a similar result below 5 K.

These behaviors are very consistent with the $\chi(T)$ curve obtained in $H=100$ Oe. That is, as T decreases from 50 K, χ increases rapidly particularly below ~20 K, suggesting the existence of localized moments. Moreover, since the $\chi(T)$ curve obtained in field-cooling (FC) mode starts to deviate from that in zero-field-cooling (ZFC) mode below ~20 K, a spin-glass-like freezing component develops with lowering T at low T. Furthermore, the fact that V_F of the magnetic phase is estimated as ~30% at 1.8 K indicates that the origin of the localized moments is not by impurities but by an intrinsic feature of KCO with $x=0.6$.

2. $K_{4/7}CoO_2$

For KCO with $x=4/7$, the ZF spectrum exhibits a slow relaxation with a broad minimum around 10 μs [see Fig. 1(c)], which is a typical behavior of a KT signal due to randomly oriented nuclear magnetic moments of K and ^{59}Co. Actually, the spectrum was well fitted by a single G^{DGKT} signal,

$$A_0 P_{ZF}(t) = A_{KT} G^{DGKT}(t, \Delta, \nu). \quad (5)$$

The LF spectrum indicates the static nature ($\nu \sim 0$) of the nuclear magnetic moments, in contrast to KCO with $x=0.6$. This implies that the fluctuation of localized moments would affect the static nature of nuclear moments in KCO with $x=0.6$; in other words, ν_2 could also be ~0 for $K_{0.6}CoO_2$. Since $\Delta(1.8\ \mathrm{K}) = 0.188 \times 10^6\ \mathrm{s}^{-1}$ and $\Delta(10\ \mathrm{K}) = 0.183 \times 10^6\ \mathrm{s}^{-1}$, Δ is found to be almost independent of T, as expected. In addition, these values are comparable to those of Δ_2 listed in Table II, suggesting the common feature of the nuclear magnetic field in K_xCoO_2 with $x \sim 0.6$. This is actually in good agreement with the metallic $\rho(T)$ curve and Pauli-PM $\chi(T)$ curve for KCO with $x=4/7$ (see Fig. 1). In contrast to KCO with $x=0.6$, in which localized moments appeared below 30 K ($V_F \sim 30\%$), the whole $x=4/7$ sample is Pauli PM even at 1.8 K. Therefore, there is a clear phase boundary (x_{cr}) of magnetic nature of KCO between $x=0.6$ and 4/7; that is, a Curie-Weiss-like metal for KCO with $x > x_{cr}$, whereas a Pauli-PM metal for $x < x_{cr}$, as in the case for NCO ($x_{cr} \sim 0.62$).[23]

3. β-$K_{0.5}CoO_2$

Only the $x=0.5$ sample exhibits clear oscillations at 1.8 K. Figure 4 shows that the Fourier transform spectrum of the ZF-μ^+SR time spectrum depends strongly on T below 55 K: above 45 K, the spectrum consists of two sharp peaks; for $20 \leqslant T < 45$ K, it splits into up to three relatively weak peaks; and below 15 K, the peak around 0.8 MHz is dominant, with two or three side peaks. This behavior is similar to that observed for single crystals of γ-$K_{\sim 0.5}CoO_2$,[1,11] γ-$Na_{0.5}CoO_2$,[13] and a polycrystalline sample of γ-$Na_{0.5}CoO_2$.[12] Indeed the ZF-μ^+SR spectrum at 1.8 K was well fitted by a combination of four oscillatory signals with a common phase and two exponentially relaxation signals. One of the latter is due to slowly fluctuating moments and the other corresponds for a "1/3 tail" caused by the AF component parallel to the initial muon spin polarization,

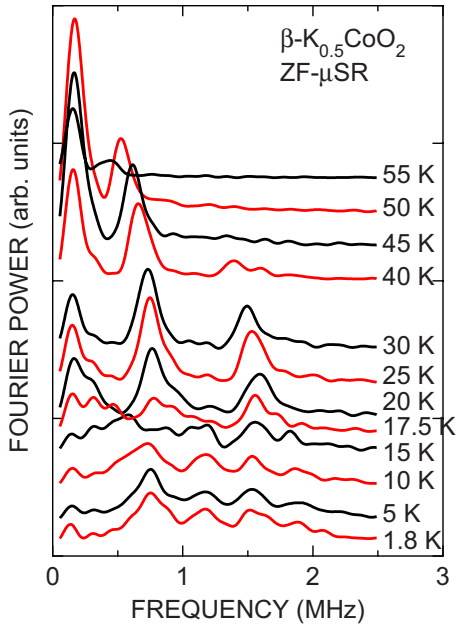

FIG. 4. (Color online) Temperature dependence of the Fourier transform of the ZF-μ^+SR time spectrum for β-$K_{0.5}CoO_2$.

$$A_0 P_{ZF}(t) = \sum_{i=1}^{4} A_{AF,i} \cos(\omega_{\mu,i} t + \phi) \exp(-\lambda_i t) + A_{slow} \exp(-\lambda_{slow} t) + A_{tail} \exp(-\lambda_{tail} t), \quad (6)$$

where ϕ is the initial phase of the precession, A_i are the asymmetries, λ_i ($i=1-4$) are exponential relaxation rates, and $\omega_{\mu,i}$ are the muon Larmor frequencies of the four signals.

Since ϕ ranges between $-10°$ and $-20°$ below 45 K, the static AF order is found to be commensurate to the crystal lattice,[19] as in the case for the γ-$K_{0.49}CoO_2$ crystal. Figure 5 shows the T dependences of (a) muon precession frequencies ($f_i \times 2\pi \equiv \omega_{\mu,i}$), (b) normalized asymmetries (N_{A_i}), (c) λ_i for the two nonoscillatory signals, (d) χ, and (e) $d\rho/dT$ for β-$K_{0.5}CoO_2$. Note that $N_{A_{tail}}$ was fixed as 1/3 in the whole T range below T_N. The complex T dependence of f_i is basically the same to that for γ-$K_{\sim 0.5}CoO_2$ (see Fig. 6), suggesting that the change in the μ^+ sites is due to charge ordering at 20 K, as is the case for γ-$Na_{0.5}CoO_2$ at 58 K.[13] That is, there are mainly four μ^+ sites below T_{CO}, whereas three sites between T_{CO} and T_N. This is qualitatively reasonable, because the number of potential minima below T_{CO}, near the CoO_2 plane where μ^+'s are located so as to bind to O^{2-} ions, is expected to be larger than that above T_{CO} due to inhomogeneous charge distribution in the charge-order state. Furthermore, according to neutron scattering experiments on γ-$Na_{0.5}CoO_2$, magnetic Bragg peaks appear below T_N and their intensity increases monotonically, i.e., order-parameter-like with decreasing T, without detectable changes at

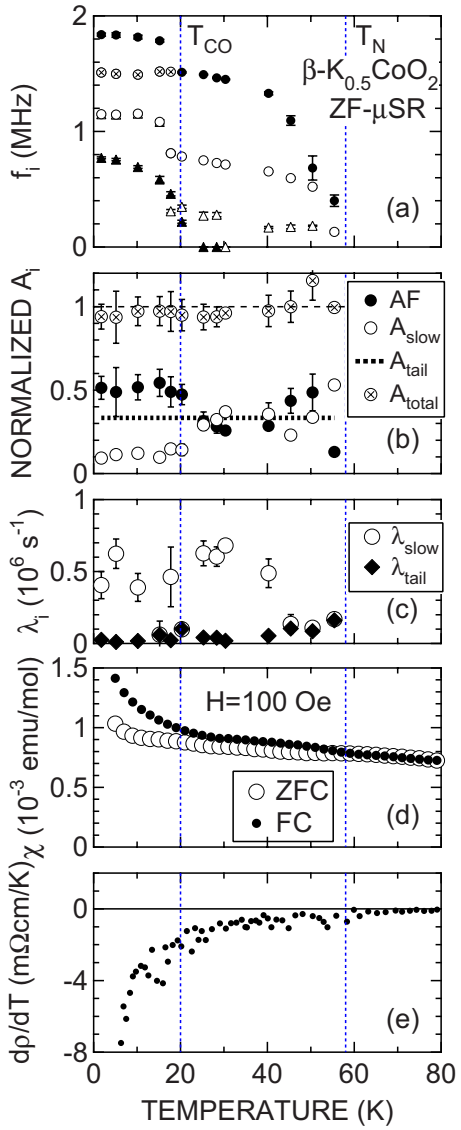

FIG. 5. (Color online) Temperature dependences of (a) muon precession frequencies ($f_i \times 2\pi \equiv \omega_{\mu,i}$), (b) normalized asymmetries $N_{A_{AF}}$, $N_{A_{slow}}$, $N_{A_{tail}}$, and $N_{A_{total}}$, where $A_{AF}=\Sigma A_{AF,i}$, $N_{A_{tail}}=1/3$, and $N_{A_{total}}=N_{A_{AF}}+N_{A_{slow}}+N_{A_{tail}}$, (c) λ_{slow} and λ_{tail}, (d) χ, and (e) $d\rho/dT$ of the $\rho(T)$ curve in Fig. 1(a) for β-$K_{0.5}CoO_2$. The data were obtained by fitting the ZF spectrum using Eq. (3). χ was measured both in FC and ZFC modes with $H=100$ Oe.

T_{CO}.[23,24] This is also supported by ^{23}Na- and ^{59}Co-NMR experiments.[23,25] Therefore, the long-range magnetic order detected by neutrons does not change at T_{CO}, while the μ^+'s experience a different field below and above T_{CO}. In order to explain this discrepancy, it is most likely that the μ^+'s change their sites below and above T_{CO}, as will be discussed in more detail later.

The normalized total asymmetry ($N_{A_{total}}=\Sigma N_{A_i}$) is almost 1 below 55 K. This means that the whole sample enters into the magnetic phase below T_N ($V_F \sim 100\%$). Here, the normalized asymmetry for the AF signals ($\Sigma A_{AF,i}$) is estimated as ~ 0.5 and $N_{A_{slow}} \sim 0.1$ below T_{CO}, although $N_{A_{AF}} \sim N_{A_{slow}} \sim 1/3$ between T_{CO} and T_N. In order to explain the decrease

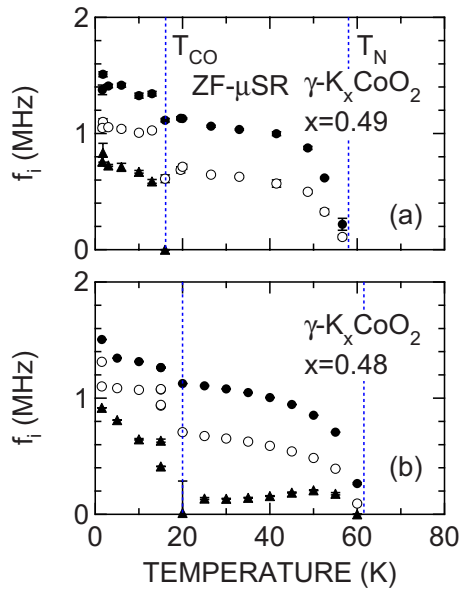

FIG. 6. (Color online) Temperature dependences of muon precession frequencies for two single crystal samples of (a) γ-$K_{0.49}CoO_2$ (Ref. 1) and (b) γ-$K_{0.48}CoO_2$ (Ref. 11). The former is metallic down to 2 K, while the latter exhibits a metal-insulator transition at 20 K. The microscopic magnetic nature detected by μ^+SR is, however, similar for these two crystals, suggesting that the charge order occurs even in the former metallic crystal on the order of the muon spatial scale sensitivity, i.e., within the few nearest neighbors.

in $N_{A_{AF}}$ above T_{CO}, we assume that the AF structure of the CoO_2 plane in β-$K_{0.5}CoO_2$ is similar to that of γ-$Na_{0.5}CoO_2$, i.e., in the alternating arrangement of $Co^{(3.5-\delta)+}$ ($S=0$) and $Co^{(3.5+\delta)+}$ ($S=1/2$) chains along the b axis, the neighboring $Co^{(3.5+\delta)+}$ spins, which are parallel to the chain (a axis), are coupled antiferromagnetically (see Fig. 7).[24,25]

According to the electrostatic potential calculation on γ-$Na_{0.5}CoO_2$, the μ^+'s are most likely to sit above O1 (below O2) ions, i.e., at site 1 with $z \sim 0.18$ (and site 2 with $z \sim -0.18$), where muons are ~ 1 Å away from the O ions. Above T_{CO}, site 1 is electrostatically equivalent to site 2. The

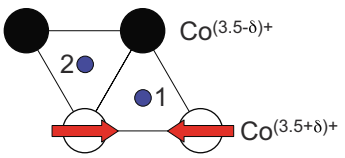

FIG. 7. (Color online) AF and charge-order states of the CoO_2 plane with the average Co valence=3.5, determined by neutron and NMR for γ-$Na_{0.5}CoO_2$ (Refs. 24 and 25). δ is estimated below 0.2. Arrows represent the AF-coupled Co moment, large circles Co ions, and small circles O ions. The Co ions are at $z=0$ and O1 ions at $z=0.09$ (O2 ions at $z=-0.09$). The μ^+'s are most likely to sit above O1 (below O2) ions, i.e., at site 1 with $z \sim 0.18$ (site 2 with $z \sim -0.18$), where the μ^+'s are ~ 1 Å away from the O ions. Above T_{CO}, site 1 is electrostatically equivalent to site 2. The K (Na) ions are located above either Co or O ions at $z=0.25$ each with occupancy of 0.25.

K (Na) ions can be located above either Co or O ions with $z=0.25$. When K (Na) ion is above the top-right Co ion, it forces the μ^+ at site 1 to shift its position toward the middle of the bottom edge of the triangle, while the K (Na) ion above the O2 ion will shift the μ^+ position at site 1 toward the bottom-right Co ion. Therefore, although site 1 is crystallographically unique and equivalent to site 2 above T_{CO}, several crystallographically inequivalent μ^+ sites exist around site 1 (site 2) in the lattice depending on the position and occupancy of K (Na) ions. The μ^+'s at and/or around site 1, which is nearer to the AF-coupled chain than site 2, are expected to detect a static AF field, whereas the μ^+'s at and/or around site 2, a weak and/or random field. As a result, almost 1/3 of the μ^+'s $[=(A_{total}-A_{tail})/2]$ provide the A_{slow} signal.

Below T_{CO}, on the other hand, in order to keep local charge neutrality, the K (Na) ions are thought to change their position slightly to increase (decrease) the density distribution around the $Co^{(3.5-\delta)+}$ ($Co^{(3.5+\delta)+}$) stripe. The majority of the μ^+'s are therefore likely to sit at and/or around site 1, resulting in larger $N_{A_{AF}}$ (~ 0.5) and f_i's below T_{CO} than those above T_{CO} ($\sim 1/3$). This explanation is reasonable and qualitatively consistent with the experimental result. In order for further understanding the detail of the changes in f_i's at T_{CO}, we, however, need to know the precise structural information as a function of T especially below T_N and T_{CO}, although such data are currently unavailable. In particular, since μ^+'s feel a repulsive force from the K^+ ions as described above, the accurate position and occupancy of the K^+ ions are crucial information to determine and/or calculate the origin of the four f_i's seen in Fig. 5(a).

The difference in the magnitude between λ_{slow} and λ_{tail} is also consistent with the above discussion. This is because the A_{slow} signal is considered to come from the μ^+'s located near the CoO_2 planes. Even for the μ^+'s located at site 2, muon spins are still depolarized by the AF-coupled Co moments in the neighboring chains.

The $\chi(T)$ curve obtained in FC mode $[\chi_{FC}(T)]$ with $H=100$ Oe indicates a small change in slope at T_N, and the difference between the $\chi_{FC}(T)$ and $\chi_{ZFC}(T)$ curves becomes larger below around T_{CO} than that above T_{CO}, suggesting the appearance of a ferrimagnetic component, if the AF structure is the same to that for γ-$Na_{0.5}CoO_2$. On the other hand, as T decreases from 80 K, the $d\rho/dT(T)$ curve starts to decrease from 0 below around T_N, monotonically decreases down to T_{CO}, and then rapidly decreases with further decreasing T.

4. Comparison with γ-$K_{0.5}CoO_2$

Referring back to Figs. 5(a) and 6, we wish to emphasize again that the magnetic nature of β-$K_{0.5}CoO_2$ is very similar to that of γ-$K_{\sim 0.5}CoO_2$. The arrangement of the Co ions along the c axis in the γ phase is different from that in the β phase; in the former, the Co ions are located at the same (x,y) position to those in the neighboring CoO_2 planes due to the *A-B-B-A* arrangement of the O ions, whereas in the latter, at the center of the Co triangular lattice due to the *A-B-B-C-C-A* arrangement of the O ions. This means that, although the interlayer distance for the γ phase is almost equivalent to that for the β phase, the interaction between the layers in the β phase is negligibly small compared with that in the γ phase. The interplane interaction is therefore most likely unessential for forming the AF order in $K_{0.5}CoO_2$. This conclusion is also supported by the fact that β-$Na_{0.5}CoO_2$ exhibits two successive transitions (T_N and T_{CO}) at nearly same temperatures for γ-$Na_{0.5}CoO_2$.[2,26]

Besides a small deviation of T_N and T_{CO} with x and/or stacking sequence, the main difference between the two phases is the magnitude of the highest f (f_{max}); that is, $f_{max}(T\rightarrow 0\ \mathrm{K})=1.8$ MHz for the β phase, whereas $f_{max}(T\rightarrow 0\ \mathrm{K})=1.5$ MHz for the γ phase. If we ignore the effect of K^+ ions on the μ^+ sites, dipole field calculations provide the ratio of f_{max} between the β and the γ phase as ~ 1.02, being too small for explaining the experimental results. The μ^+'s at and/or around site 1 are therefore likely to shift toward magnetic Co ions by about 6% in the β phase, compared with the case in the γ phase.

According to recent neutron and x-ray diffraction analyses on γ-$K_{0.5}CoO_2$ at high T, a structural transition from a high-T hexagonal phase ($P6_3/mmc$) to a low-T orthorhombic phase ($Pnmm$) occurs at around 550 K due to K order,[2] as in the case for γ-$Na_{0.5}CoO_2$.[27,28] Similar K order is also observed for β-$K_{0.5}CoO_2$.[29] Hence, in spite of the K order in $K_{4/7}CoO_2$, γ-$K_{0.5}CoO_2$, and β-$K_{0.5}CoO_2$, the former is Pauli PM even at 1.8 K but the latter two are AF below ~ 60 K. This implies that the K order is not directly connected to the formation of magnetic order in the CoO_2 plane. These results suggest that the magnetic nature of the CoO_2 plane is approximately understandable by considering the physics only on one CoO_2 plane.

IV. SUMMARY

Three K_xCoO_2 samples with $x=0.6$, 4/7, and 0.5 have been investigated by means of muon spin spectroscopy in order to know the change in local magnetic nature with x near quarter filling ($x=1/2$). For the γ-$K_{0.6}CoO_2$ sample, localized moments appear below 20 K but do not order even at 1.8 K. Combining this with the increase in χ at low T, γ-$K_{0.6}CoO_2$ is thought to be a Curie-Weiss metal. On the other hand, the absence of fast relaxations (nor rotations) in the ZF-μ^+SR spectrum shows that the γ-$K_{4/7}CoO_2$ sample, for which the K order enlarges the lattice by seven times in the c plane, is entirely Pauli paramagnetic down to 1.8 K. The phase boundary between the CW-PM metal and Pauli-PM metal is therefore found to exist just below $x=0.6$.

Only for the β-$K_{0.5}CoO_2$ sample the quasistatic AF order appears below 58 K ($=T_N$), and, moreover, the whole sample enters into the AF phase below T_N, as in the case for γ-$K_{0.5}CoO_2$. Considering the structural difference between β and γ phases, it is found that the interplane (three-dimensional) interaction is not essential for the AF order of the CoO_2 plane. In addition, the K order is thought to be not a significant factor for determining the magnetic nature of the CoO_2 plane, based on the comparison with γ-$K_{4/7}CoO_2$. These indicate that the spin and charge orders are intrinsic feature of the CoO_2 plane.

ACKNOWLEDGMENTS

This work was performed at the Swiss Muon Source, Paul Scherrer Institut, Villigen, Switzerland. We thank the staff of PSI for help with the μ^+SR experiments. We also appreciate J. H. Brewer of the University of British Columbia and E. J. Ansaldo of TRIUMF for discussion. Y.I. and J.S. are partially supported by the KEK-MSL Inter-University Program for Oversea Muon Facilities. M.B. and C.D. are supported by the Council of Région Aquitaine, CNRS and the French National Research Agency (ANR). This work is also supported by Grant-in-Aid for Scientific Research (B), 19340107, MEXT, Japan.

*e0589@mosk.tytlabs.co.jp

[1] J. Sugiyama, H. Nozaki, Y. Ikedo, K. Mukai, J. H. Brewer, E. J. Ansaldo, G. D. Morris, D. Andreica, A. Amato, T. Fujii, and A. Asamitsu, Phys. Rev. Lett. **96**, 037206 (2006).

[2] H. Watanabe, Y. Mori, M. Yokoi, T. Moyoshi, M. Soda, Y. Yasui, Y. Kobayashi, M. Sato, N. Igawa, and K. Kakurai, J. Phys. Soc. Jpn. **75**, 034716 (2006).

[3] D. Qian, L. Wray, D. Hsieh, D. Wu, J. L. Luo, N. L. Wang, A. Kuprin, A. Fedorov, R. J. Cava, L. Viciu, and M. Z. Hasan, Phys. Rev. Lett. **96**, 046407 (2006).

[4] I. Terasaki, Y. Sasago, and K. Uchinokura, Phys. Rev. B **56**, R12685 (1997).

[5] J. Sugiyama, H. Itahara, J. H. Brewer, E. J. Ansaldo, T. Motohashi, M. Karppinen, and H. Yamauchi, Phys. Rev. B **67**, 214420 (2003); J. Sugiyama, J. H. Brewer, E. J. Ansaldo, H. Itahara, T. Tani, M. Mikami, Y. Mori, T. Sasaki, S. Hébert, and A. Maignan, Phys. Rev. Lett. **92**, 017602 (2004); J. Sugiyama, J. H. Brewer, E. J. Ansaldo, B. Hitti, M. Mikami, Y. Mori, and T. Sasaki, Phys. Rev. B **69**, 214423 (2004).

[6] S. P. Bayrakci, I. Mirebeau, P. Bourges, Y. Sidis, M. Enderle, J. Mesot, D. P. Chen, C. T. Lin, and B. Keimer, Phys. Rev. Lett. **94**, 157205 (2005).

[7] L. M. Helme, A. T. Boothroyd, R. Coldea, D. Prabhakaran, D. A. Tennant, A. Hiess, and J. Kulda, Phys. Rev. Lett. **94**, 157206 (2005).

[8] M. L. Foo, Y. Wang, S. Watauchi, H. W. Zandbergen, T. He, R. J. Cava, and N. P. Ong, Phys. Rev. Lett. **92**, 247001 (2004).

[9] K. Takada, H. Sakurai, E. Takayama-Muromachi, F. Izumi, R. A. Dilanian, and T. Sasaki, Nature (London) **422**, 53 (2003).

[10] C. Delmas, C. Fouassier, and P. Hagenmuller, J. Solid State Chem. **13**, 165 (1975).

[11] J. Sugiyama, Y. Ikedo, P. L. Russo, K. Mukai, H. Nozaki, J. H. Brewer, E. J. Ansaldo, K. H. Chow, D. Andreica, A. Amato, T. Fujii, A. Asamitsu, K. Ariyoshi, and T. Ohzuku, Proceedings of the 14th Semiconducting and Insulating Materials Conference, 2007 (unpublished).

[12] P. Mendels, D. Bono, J. Bobroff, G. Collin, D. Colson, N. Blanchard, H. Alloul, I. Mukhamedshin, F. Bert, A. Amato, and A. D. Hillier, Phys. Rev. Lett. **94**, 136403 (2005).

[13] J. Sugiyama (unpublished).

[14] J. Sugiyama, H. Nozaki, J. H. Brewer, E. J. Ansaldo, G. D. Morris, and C. Delmas, Phys. Rev. B **72**, 144424 (2005).

[15] K. Mukai, Y. Ikedo, H. Nozaki, J. Sugiyama, P. L. Russo, K. Nishiyama, D. Andreica, A. Amato, J. H. Brewer, E. J. Ansaldo, K. H. Chow, K. Ariyoshi, and T. Ohzuku, Phys. Rev. Lett. **99**, 087601 (2007).

[16] M. Blangero, R. Decourt, D. Carlier, G. Ceder, M. Pollet, J.-P. Doumerc, J. Darriet, and C. Delmas, Inorg. Chem. **44**, 9299 (2005).

[17] C. Fouassier, G. Matejka, J.-M. Reau, and P. Hagenmuller, J. Solid State Chem. **6**, 532 (1973).

[18] M. Blangero (private communication); the KCO samples with x between 0.5 and 0.6 were found to be a mixture of $K_{0.5}CoO_2$ and $K_{0.6}CoO_2$, except for $K_{4/7}CoO_2$.

[19] G. M. Kalvius, D. R. Noakes, and O. Hartmann, in *Handbook on the Physics and Chemistry of Rare Earths*, edited by K. A. Gschneidner, Jr., L. Eyring, and G. H. Lander (North-Holland, Amsterdam, 2001), Vol. 32, Chap. 206.

[20] Y. Ikedo, J. Sugiyama, H. Nozaki, H. Itahara, J. H. Brewer, E. J. Ansaldo, G. D. Morris, D. Andreica, and A. Amato, Phys. Rev. B **75**, 054424 (2007).

[21] F. C. Chou, J. H. Cho, and Y. S. Lee, Phys. Rev. B **70**, 144526 (2004).

[22] G. Lang, J. Bobroff, H. Alloul, P. Mendels, N. Blanchard, and G. Collin, Phys. Rev. B **72**, 094404 (2005).

[23] M. Yokoi, T. Moyoshi, Y. Kobayashi, M. Soda, Y. Yasui, M. Sato, and K. Kakurai, J. Phys. Soc. Jpn. **74**, 3046 (2005).

[24] G. Gašparović, R. A. Ott, J.-H. Cho, F. C. Chou, Y. Chu, J. W. Lynn, and Y. S. Lee, Phys. Rev. Lett. **96**, 046403 (2006).

[25] J. Bobroff, G. Lang, H. Alloul, N. Blanchard, and G. Collin, Phys. Rev. Lett. **96**, 107201 (2006).

[26] L. Viciu, J. W. G. Bos, H. W. Zandbergen, Q. Huang, M. L. Foo, S. Ishiwata, A. P. Ramirez, M. Lee, N. P. Ong, and R. J. Cava, Phys. Rev. B **73**, 174104 (2006).

[27] H. W. Zandbergen, M. L. Foo, Q. Xu, V. Kumar, and R. J. Cava, Phys. Rev. B **70**, 024101 (2004).

[28] Q. Huang, M. L. Foo, J. W. Lynn, H. W. Zandbergen, G. Lawes, Y. Wang, B. H. Toby, A. P. Ramirez, N. P. Ong, and R. J. Cava, J. Phys.: Condens. Matter **16**, 5803 (2004).

[29] M. Blangero (unpublished).